Analysis of the Stiffness of Modular Reconfigurable Parallel Robot with Four Configurations

Qisheng Zhang, Ruiqin Li(✉), Qing Li, and Jingjing Liang

School of Mechanical and Power Engineering, North University of China, Taiyuan 030051, China
{1020709642,695558745,944719179}@qq.com, liruiqin@nuc.edu.cn

Abstract. This paper studies the static stiffness of a kind of Modular Reconfigurable Parallel robot (MRP robot for short). The MRP robot can be reconstituted to four different configurations. The 3D entity models of the MRP robot of all configurations are established by UG software, according to the modular modeling method and certain simplified rules. The stiffness model of the MRP robot is established. The factors affecting stiffness of the MRP robot are obtained. The static stiffness and stress distribution of the MRP robot are obtained with different forces in the initial position of various configurations by using ANSYS. The static stiffness in z direction (perpendicular to the static base) of each configuration is larger than the static stiffness in x and y directions (in the static base). This shows that the main stiffness is located in z direction. While the stiffness in x, y directions are close to each other. The main stiffness of four kinds of configurations is different. The main stiffness of 6-SPS configuration is significantly greater than that of other three kinds of configurations. The weaker links of the MRP robot are related to the position of the hinges and the connecting position of the moving platform and the screw. The overall stiffness of the MRP robot can be obviously improved by increasing the stiffness of the module which has great influence on the stiffness. The results provide a theoretical basis for the design of the MRP robot.

Keywords: Modular reconfigurable robot (MRP) · Parallel robot · Configuration · Stiffness

1 Introduction

Modular Reconfigurable Parallel robot (MRP robot for short) consists of a series of modules such as joint, connecting rod, the end-effector with different size and functional characteristics. The MRP robot can be changed to different configurations through simple and quick assembly and disassembly among modules in the way of building blocks [1]. The MRP robot has the flexibility characteristic. It can better meet the demands of configuration variation. However, stiffness, precision and ratio of load to self-weight of the MRP robot are not satisfactory which are limited by its own structure. Therefore, it is an important research topic to make the MRP robot have better reconfigurable ability, strong processing capacity and good operating performance.

The static stiffness is one of the important performance indices of parallel robot. It is beneficial to improve the efficiency of the robot, machining accuracy and surface

N. Kubota et al. (Eds.): ICIRA 2016, Part I, LNAI 9834, pp. 198–209, 2016.
DOI: 10.1007/978-3-319-43506-0_17

quality by improving the static stiffness of robot. Many studies on the stiffness of the parallel robot have been done. Many methods are adopted including finite element analysis method, analytical model of static stiffness and static stiffness performance analysis, etc. [2]. The stress and deformation at the end of parallel robot is not simple linear superposition of the deformation produced by limbs and frame, but a coupling nonlinear function with many limbs. Therefore, it is much more complex to analyze the static stiffness of parallel robot. Some simplification and optimization of the model have been done before modeling when analytic method and performance analysis used to analyze static stiffness. However, these simplification methods can't accurately solve the stiffness of the robot and the error is large. In view of the complexity of geometric shape and boundary conditions of mechanical structure, finite element analysis method is usually used to modeling and calculating the stiffness of the robot [3].

In recent years, many scholars have studied the stiffness of parallel manipulators with various configurations by using finite element method. Wang Nan et al. [4] have made static and dynamic characteristics analysis of a 3-DOF 3-SPS/S type parallel machine tool, and gained the static stiffness performance by using finite element analysis software. Yan Binkuan et al. [5] have made static analysis of a 3-SPS/S type parallel machine tool, got the stiffness characteristics in each direction and characteristics of the first 6 order natural frequency. Li Xingshan et al. [6] have set up 3D model of 2TPT-PTT hybrid parallel machine tool, and built finite element model of this type parallel machine tool in workbench, studied the static stiffness with different forces. The results indicate that the static stiffness in z direction is larger than it in x and y directions and the hooke joint and parallel mechanism are the important factors affecting the stiffness of the whole mechanism. Chen Guangwei et al. [7] have established finite element model of whole static stiffness for a new type gantry plane parallel mechanism of parallel machine tool, and got distribution of stiffness of moving platform under the generalized workspace. Li et al. [8] established an improved 3-PRC model of flexible parallel manipulator mechanism, and analyzed stiffness and static mechanics of the model by using ANSYS software, gained the stiffness change trend of related to structural parameters. All above researches on the parallel mechanism are based on the finite element software, while all elastic of elastic parts is ignored such as frame, hinge, ball screw etc.

In view of the fact that ignoring elastic of transmission system in the process of finite element analysis such as hinge, screw and bearings etc. lead to larger errors, this paper will establish the stiffness model for an existing MRP robot experiment platform. The strategy to simplify 3D model of MRP robot is proposed. In Ansys Workbench platform, the overall static stiffness of the MRP robot with four configurations at initial position will be analyzed.

2 Structure and Parameters of the MRP Robot

2.1 Structure Characteristics of the MRP Robot

The MRP robot can change into four different configurations, through changing connection modes of moving platform, linkage, ball screw pairs, hooke hinge into different

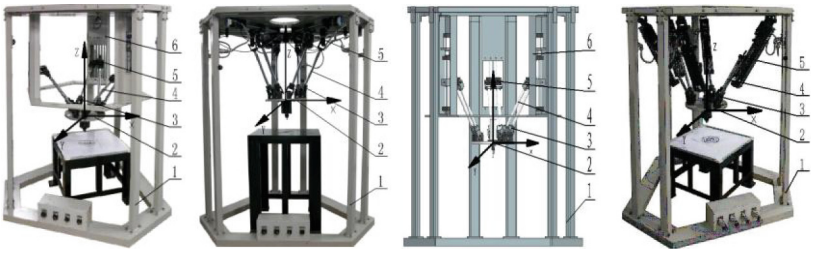

Fig. 1. Four kinds of different configurations of the MRP robot

ones, as shown in Fig. 1(a) ~ (d), which are called 6-PSS slider type, 6-PSS scissors type, 3-Delta slider type, 6-SPS telescopic type, respectively.

As shown in Fig. 1(a), 6-PSS slider type parallel robot consists of body support, six kinematic chains and driver module. Six pairs of driver module are fixed into three group vertical pillars. Each pillar contains 2 sets of driver modules. Each driver module connects to a set of linkage, and at linage end connects to the moving platform.

As shown in Fig. 1(b), 6-PSS scissors type parallel robot configuration consists of six sets of driver modules which are fixed on the top base plate. Each driver module connects to a set of linkage, and working platform connects to the end of linkage.

As shown in Fig. 1(c), 3-Delta slider type parallel robot consists of body support and three kinematic chains and driver module. Under this kind of configuration, three sets of driver modules are fixed in vertical pillar, each driver module connects two sets of linkage, which forms parallelogram mechanism, and the end of linkage connects to moving platform.

As shown in Fig. 1(d), when change into 6-SPS telescopic type parallel robot configuration, one end of six set of driver modules are fixed on the top base plate, the other side connect to linkage with parts of ball screw socket within the linkage, and keep the ball screw and linkage in same axis, which make the length of the linkage variable. The end of linkage connected to the moving platform. Driver modules are driven by servo motors, and it makes lead screw nut pair move, make the wire mother slide along the axis of the ball screw through cooperative movement of the linkage, drive moving platform working and achieve the desired trajectory.

2.2 Structural Parameters of the MRP Robot

The outside framework of the MRP robot is 1316 mm, the static platform constitutes of hexagon with 1156 mm circumscribed circle diameter. The diameter of the moving platform is 316 mm. The body weight is 240 kg. The work scope of prismatic pairs is limited to {-100 mm, 100 mm}. The length of the linkage is 321 mm.

3 Theoretical Basis of Stiffness Analysis

The main factor affecting the stiffness of the MRP robot is the stiffness of transmission system, when the influence of gravity of linkage and stiffness of hinge are ignored. Supposing the force applying on the center of the moving platform is $F_p = [\ F_x\ \ F_y\ \ F_z\ \ m\ ]$, m is torque, driving force is $F_d = [\ F_1\ \ F_2\ \ F_3\ ]$, the following equation can be gotten.

$$F_d = K_t \Delta l \tag{1}$$

Where, K_t is the transmission stiffness of the parallel robot. It can be expressed as

$$K_t = diag(K_{ii}),\ \ i = 1, 2, 3$$

Where, K_{ii} is the transmission stiffness of ith limb. Δl is displacement deformation along driving direction caused by transmission stiffness, corresponding with which terminal deformation is $\Delta O_p = \left[\ \Delta x\ \ \Delta y\ \ \Delta z\ \right]^T$.

Under the condition of static equilibrium, in order to make virtual displacement of drive as $\delta l = \left[\ \delta l_1\ \ \delta l_2\ \ \delta l_3\ \right]^T$, corresponding with δl make terminal deformation as $\delta O_p = \left[\ \delta x\ \ \delta y\ \ \delta z\ \right]^T$, and get:

$$\Delta l = J \Delta O_p \tag{2}$$

$$\delta l = J \delta O_p \tag{3}$$

By using the principle of virtual work, yield:

$$F^T \delta O_p = F_d^T \delta l \tag{4}$$

Substituting Eqs. (1), (2) and (3) into Eq. (4), then

$$F = J^T K_t J \cdot \Delta O_p \tag{5}$$

Let $K = J^T K_t J$, it is called the static stiffness matrix of the MRP robot. Equation (5) is the static stiffness model of the parallel robot. From Eq. (5), the stiffness matrix of the end-effector of the MRP robot consists of the stiffness of each link and the Jacobian matrix J. The Jacobian matrix changes over the position and orientation of the robot. Thus the stiffness matrix also depends on the position and orientation of the robot.

For a given position and orientation, the deformation size of the moving platform is related to the direction of the force. Static stiffness of the parallel robot can be calculated by the force F which is applied at the center of moving platform, and the displacement of the point is applied by force.

$$K = F / \Delta O_p \tag{6}$$

The static stiffness of the parallel robot in all directions can be calculated by using this method.

4 Stiffness Analysis of the MRP Robot

4.1 Modeling and Simplification Strategy of the MRP Robot

The MRP robot can change into four different configurations. Each configuration is made up of many parts. Considering the relationships among various configurations, all configurations are constituted of the same parts, components and modules, which can be gained by different combination. The method of modular modeling is used to build the model of the robot in order to make full use of the parametric modeling advantages of UG software and the modular characteristics of the mechanism. All of the components are treated as individual modules, which can be independent as a unit such as the moving platform, linkage, kinematic pair, robot body, etc.

Various configurations are built through connecting these modules to the moving platform and static platform with the aid of hooke hinges. Equivalent replacing, simplifying and modifying the model in UG software follow the following principles in order to facilitate subsequent finite element analysis.

(1) Merging all of the parts which contact to each other without relative movement. Deleting the parts which do not force or a little force, such as servo motor, screw, nut, bearing cover, etc. The influence of these parts for the whole structure can be ignored in the process of stress analysis.
(2) Deleting all the features of holes and chamfers in the parts. These features are not affect the results of stiffness analysis. However, it is very significant to occupy computer resources when dividing grid.
(3) Simplifying rules for elastic components and Hooke hinges. Under a certain position and orientation, Hooke hinge is simplified to a 2-DOF joint. The contact surface of screw and screw nut of prismatic pair are coupled which can't be ignored due to the existence of gap.

4.2 Pre-process for Finite Element Analysis

4.2.1 Defining Material Properties of the Robot Parts

The materials of driving parts and Hooke hinges are structural steel, modulus of elasticity $E = 2.09 \times 10^{11}$Pa, Poisson's ratio $\gamma = 0.269$ and density $\rho = 7890\text{kg/m}^3$. The rest parts of the parallel robot are 45 steel, modulus of elasticity $E = 2.06 \times 10^{11}$Pa, Poisson's ratio $\gamma = 0.3$ and density $\rho = 7890\text{kg/m}^3$.

4.2.2 Meshing

The meshing quality of model directly affects the precision of the calculation results and computing time. Therefore it is a key factor in finite element analysis.

The sizes of robot body and static platform are bigger compared to other parts, which has less influence on overall stiffness. Selecting 50 mm as element size. The main forced parts select 2 mm as element size such as screw and hinge. The contact areas of the parts need further refined. In general, with the increase of the number of grid, the precision of the calculation results will be improved, but the computing time will be increased.

4.2.3 Loading and Solving

According to the actual working situation of the MRP robot, robot body of each configuration is fixed to the ground. The stiffness of the MRP robot system under different configurations, different positions and orientations is different from Eq. (5). The paper studies the stiffness of the four configurations in the initial position and orientation.

Down milling type of milling cutter is usually adopted when the MRP robot of each configuration is located in the initial position and orientation. This is equivalent to a planar milling machine movement. The excitation force applied on the robot comes from milling cutter. The numerical of the milling force can be seen as amplitude of sine excitation. The calculating equation can be obtained from reference [9]. The main milling force for end milling plane can be expressed as follows.

$$F_m = 6e10^4 \times \frac{P_m}{V_m} \tag{7}$$

Where, F_m is the main milling force, i.e., the component of milling force along the main movement direction of milling cutter, N.

P_m is the milling power, KW.
V_m is the milling velocity, m/min.

In the process of milling of the four configurations, the milling power of 3-Delta type parallel robot is $P_m = 0.3$KW and the milling velocity is $V_m = 6$ m/min. Thus $F_m = 3000$N can be obtained by using Eq. (7). The milling power of other configurations is $P_m = 0.6$KW and the milling velocity is $V_m = 6$m/min. Thus $F_m = 6000$N can be obtained by using Eq. (7).

$$\begin{aligned} F_x &= 0.35F_m \\ F_y &= 0.525F_m \\ F_z &= 0.9F_m \end{aligned} \tag{8}$$

The component forces F_x, F_y and F_z of the milling force F_m along x, y and z direction of each configuration can be obtained, respectively by substituting F_m from Eq. (7) into Eq. (8). The milling force F_m along x, y, z direction are applied to the center of the moving platform. The component forces of 3-Delta configuration are $F_x = 1050$N, $F_y = 1575$N and $F_z = 2700$N. The component forces of other configurations are $F_x = 2100$N, $F_y = 3150$N, $F_z = 5400$N.

4.3 Results Analysis

Four kinds of different configurations are imported into ANSYS Workbench platform, respectively. The total contour of displacement and stress are gained of each configurations of the MRP robot at the initial position and orientation, which is gotten by applying the forces along *x, y, z* axis direction, as shown in Figs. 2, 3, 4 and 5.

4.3.1 Results of Four Kinds of Configurations

Figure 2 shows contours of displacement and stress at center of the moving platform when the force $F_x = 2100$ N, $F_y = 3150$ N, $F_z = 5400$ N is applied at the center of the moving platform, respectively for 6-PSS slider type configuration. Figure 2(a) and (b) shows the stress and displacement contours, respectively when the force $F_x = 2100$ N is applied at the center of the moving platform along x axis direction. Figure 2(c) and (d) shows the stress and displacement contours, respectively when the force $F_y = 3150$ N is applied at the center of the moving platform along y axis direction. Figure 2(e) and (f) shows the stress and displacement contours, respectively when the force $F_z = 5400$ N is applied at the center of the moving platform along z axis direction.

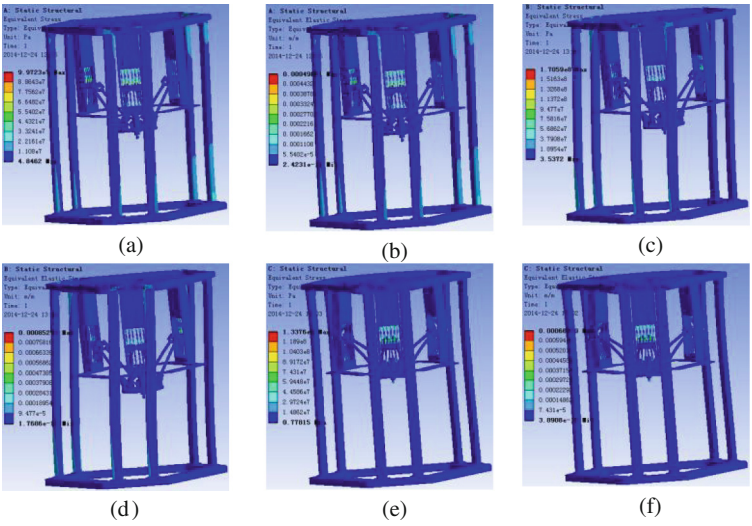

Fig. 2. Displacement and stress of 6-PSS slider configuration

Figure 3 shows contours of displacement and stress at mid-point of moving platform on the condition that the force $F_x = 2100$ N, $F_y = 3150$ N, $F_z = 5400$ N is applied at center of moving platform respectively under 6-PSS scissors type configuration. Figure 3(a) and (b) shows the stress and displacement contours, respectively on the condition that the force $F_x = 2100$ N is applied in the midpoint of working platform along x axis direction. Figure 3(c) and (d) shows the stress and displacement contours, respectively on the condition that the force $F_y = 3150$ N is applied in the midpoint of working platform along y axis direction. Figure 3(e) and (f) shows the stress and

displacement contours respectively on the condition that the force $F_z = 5400$ N is applied in the midpoint of working platform along z axis direction.

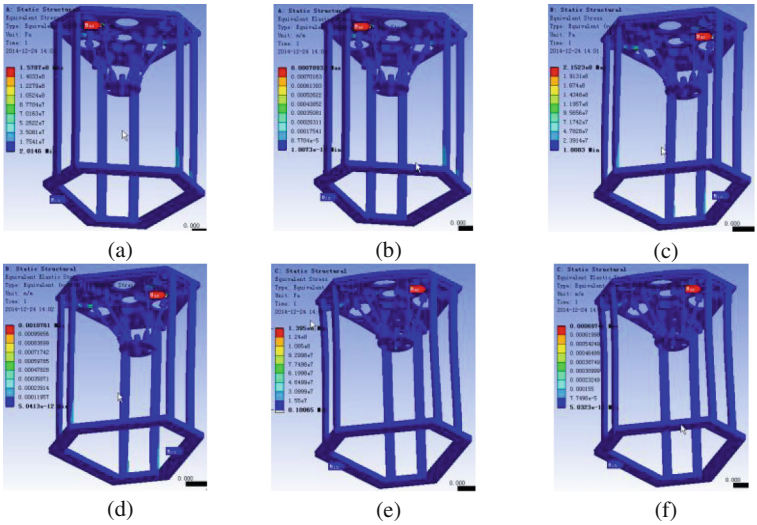

Fig. 3. Displacement and stress of 6-PSS scissors configuration.

Figure 4 shows contours of displacement and stress at mid-point of moving platform on the condition that the force $F_x = 1050$ N, $F_y = 1575$ N, $F_z = 2700$ N is applied at center of moving platform, respectively under 3-Delta type parallel robot configuration.

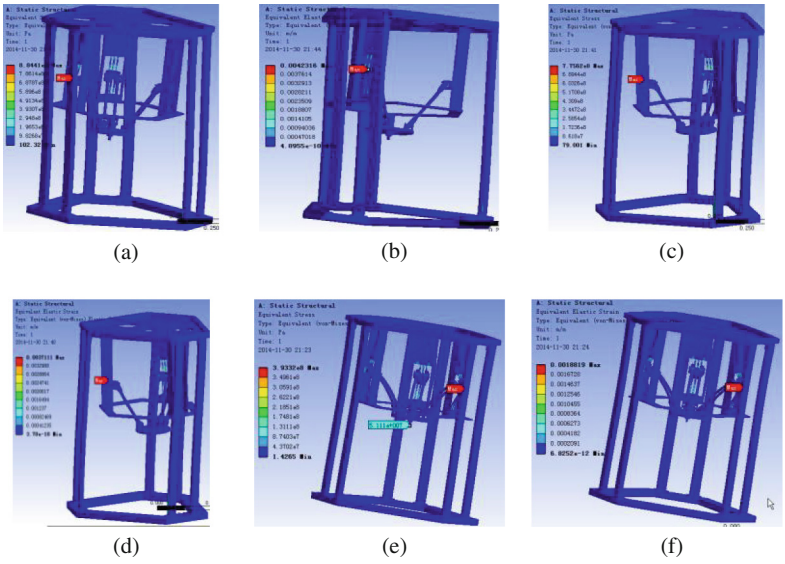

Fig. 4. Displacement and stress of 3-Delta configuration

Figure 5 shows contours of displacement and stress at mid-point of moving platform on the condition that the force $F_x = 2100$ N, $F_y = 3150$ N, $F_z = 5400$ N is applied at center of moving platform, respectively under 6-SPS telescopic type parallel robot configuration.

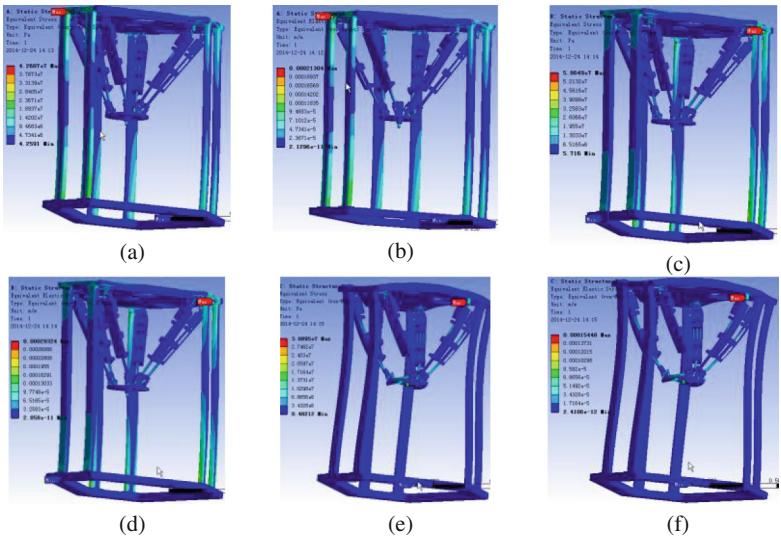

Fig. 5. Displacement and stress of 6-SPS telescopic configuration

4.3.2 Stiffness of Four Kinds of Configurations

Under four different configurations in Fig. 1, the whole deformation (denoted as Δ) and stress values, the deformation values of midpoint of moving platform (denoted as $U_x/U_y/U_z$ in x, y, z direction, respectively), the maximum stress ($\sigma_{\max}$) and the displacement values of the maximum deformation are obtained along x, y, z directions at the center of the moving platform (denoted as $\delta_{x\max}$, $\delta_{y\max}$, $\delta_{z\max}$, respectively). Then the parts and location with weak stiffness can be determined. Thus the value of static stiffness can be obtained by substituting the gained values into Eq. (6), as shown in Table 1.

4.3.3 Summary of Analysis

From calculating and analyzing, the following results can be obtained.

(1) For the same configuration at initial position and orientation, the stiffness along three axes of the static coordinate system is different. The stiffness in x and y direction are similar to each other. However, the stiffness in z direction is an order of magnitude larger than that in x, y directions. The stiffness in z direction is called main stiffness, which are the characteristics of the parallel mechanism.

(2) For four kinds of different configurations, the orders of magnitude in each direction are the same, but the values of the stiffness are different. Among all the main stiffness of all the four configurations, 6-SPS telescopic type has the largest stiffness, while 3-Delta type has the smallest stiffness. The difference between 6-PSS scissors type and

Table 1. Deformation and stiffness of the MRP robot under the different forces

Configuration	Force /N	Δ_{max} /e−5 m	σ_{max} /e7 pa	δ_{xmax} /e−5 m	δ_{ymax} /e−5 m	δ_{zmax} /e−5 m	$U_x/U_y/U_z$ /e−6 m	Stiffness /e5 N/m
6-PSS Slider	$F_x = 2100$	178	9.97	178	13.1	15.0	1780/−2.5/12.3	10.8
	$F_y = 3150$	268	17.1	18.0	268	23.4	−4.37/2680/17.8	11.8
	$F_z = 5400$	43.5	13.3	25.1	26.8	43.5	1.99/1.16/435	124
6-PSS Scissors	$F_x = 2100$	191	15.7	191	3.01	36.2	1890/−1.95/−8.54	11.1
	$F_y = 3150$	286	21.5	3.99	286	50.7	1.78/2830/43.9	11.1
	$F_z = 5400$	52.0	14.0	7.64	12.7	51.4	−23.1/71.5/511	106
3-Delta Slider	$F_x = 1050$	107	8.26	107	9.75	12.2	1070/−1.57/5.84	9.81
	$F_y = 1575$	160	13.4	160	20.2	61.0	−2.36/1600/8.65	9.84
	$F_z = 2700$	31.6	11.0	18.6	21.5	31.6	0.725/0.587/316	854
6-SPS Telescopic	$F_x = 2100$	137	4.26	137	3.95	8.27	1290/−4.04/2.11	1.63
	$F_y = 3150$	206	5.86	2.94	206	13.8	−1.03/1950/3.06	1.62
	$F_z = 5400$	9.28	3.09	4.02	5.06	9.27	1.94/1.7/92.8	582

6-PSS slider type has little difference. 6-SPS telescopic type parallel robot has a wider application range. For 3-Delta type configuration, each kinematic pair need to drive two links, which is made up of ball screw and have a relative smaller stiffness. It is consistent with the actual situation. For 6-SPS telescopic type configuration, a steel plate is added at the bottom of the mobile pairs, which caused increasing of the overall stiffness. While under others configurations, ball screw with larger deformation is just fixed at the bottom of the mobile pairs. Therefore, it is helpful to enhance the overall stiffness of the robot system by improving the stiffness of modules which have large influence on stiffness.

(3) The location with the maximum deformation under four configurations is obtained. For 6-SPS telescopic type configuration, the largest deformation locate at the areas, where is hooke joint that installed on fixed platform connecting to telescopic rod mobile pairs. And the stiffness there is relatively smaller, it is weaker links of this kind of configuration. Thus the hinge stiffness will affect the stiffness of the configuration. By analyzing the location with the maximum deformation of other configurations, the maximal displacement occurs at the position that screw of motion pair and sliding platform connecting areas, where is also weak link of the robot. The deformation of linkage and frame is small can be neglected under all four configurations. Under each configuration, the smallest deformation is at upper parts, while it is large at the lower parts. It is increasing gradually from top to down. The deformation trend is in accordance with the actual working situation. The analysis results are reasonable.

(4) The maximum stress is 215 MPa but still far less than the allowable stress of the material. The machine will not damage in actual processing conditions under each configuration. Therefore, the design is reasonable. The maximum stress occurs in the position with smaller stiffness. Thus, it is necessary to strengthen some weak parts.

5 Conclusions

The 3D entity models of the MRP robot under four different configurations are built by using UG software according to certain rules. The finite element analysis is carried out in ANSYS Workbench software. The deformation data, distribution, change regular of stress and strain of the MRP robot under four different configurations are gained when the robot is applied by external forces in x, y and z direction. The conclusions can be drawn as follows.

(1) The stiffness along the main stiffness direction is one order of magnitude larger than the other directions under various configurations. There is only very small difference between the other two directions.
(2) For the MRP robot, the stiffness in all directions is varied from each other under different configurations. The stiffness of the MRP robot can be improved by improving the stiffness of modules.
(3) The weaker link of the MRP robot is different from each other for varied configurations. All of which is relevant to the hinge, screw and the position connecting to sliding platform. Therefore, the stiffness of hinge and the screw prismatic pairs will affect the overall stiffness of the MRP robot. The weakness of each configuration at initial position is found out, which is in accordance with the actual situation.
(4) Under 6-SPS telescopic configuration, a steel plate is added to the bottom of prismatic pairs which consist of telescopic rods, and the main stiffness of this configuration is greatly improved. Therefore, the overall stiffness of the MRP robot can be significantly enhanced by improving the stiffness of modules which has large influence on stiffness.

The results provide a theoretical basis to design, improve and optimize the robot structure in the future.

Acknowledgements. The authors gratefully acknowledge the financial and facility support provided by the National Natural Science Foundation of China (Grant No. 51275486).

References

1. Jiang, Y., Wang, H., Pan, X., et al.: Autonomous online identification of configurations for modular reconfigurable robot. Chin. J. Mech. Eng. **47**(15), 17–24 (2011). (in Chinese)
2. Ai, Q., Huang, W., Zhang, H., et al.: Review of stiffness and statics analysis of parallel robot. Adv. Mech. **42**(5), 583–592 (2012). (in Chinese)
3. Wei, Y., Wang, Z.: Finite element analysis on the stiffness of the structure of parallel machine tool. Mach. Electron. **10**(4), 16–19 (2004). (in Chinese)
4. Wang, N., Zhao, C., Gao, P., et al.: Parallel manipulator 3-SPS/S static and dynamic stiffness performance study. Mach. Des. Manuf. **8**, 213–215 (2013). (in Chinese)
5. Yan, B., Zhang, N.: 3-SPS-S 3-DOF parallel mechanism static and dynamic characteristics analysis. Mech. Res. Appl. **26**(3), 35–36 (2013). (in Chinese)
6. Li, X., Cai, G.: Static stiffness analysis of hybrid parallel machine tools based on workbench. Manuf. Technol. Mach. Tool (4), 60–62 (2011). (in Chinese)

7. Chen, G., Wang, J.: The finite element analysis and optimization of static stiffness of a new parallel kinematic machine. Mach. Des. Manuf. (12), 4–6 (2006). (in Chinese)
8. Li, Y.M., Xu, Q.S.: Stiffness and statics analysis of a compact 3-PRC parallel micromanipulator for micro/nano scale manipulation. In: IEEE International Conference on Robotics and Biomimetics, Sanya, China, pp. 59–64 (2007)
9. Shanghai association of metal cutting technology. Metal cutting manual. Shanghai science and technology Press, Shanghai (2004). (in Chinese)